

Phase-Resolved Nonlinear Response of a Two-Dimensional Electron Gas under Femtosecond Intersubband Excitation

C. W. Luo,^{1,*} K. Reimann,^{1,†} M. Woerner,¹ T. Elsaesser,¹ R. Hey,² and K. H. Ploog²

¹Max-Born-Institut für Nichtlineare Optik und Kurzzeitspektroskopie, 12489 Berlin, Germany

²Paul-Drude-Institut für Festkörperelektronik, 10117 Berlin, Germany

(Received 7 July 2003; published 30 January 2004)

Strong electric-field transients resonant to intersubband transitions in *n*-type modulation-doped GaAs/AlGaAs quantum wells induce coherent Rabi oscillations, which are demonstrated by a phase-resolved measurement of the light emitted by the sample. The time evolution of the intersubband polarization is influenced by Coulomb-mediated many-body effects. The subpicosecond period and the phase of the Rabi oscillations are controlled by the properties of the midinfrared driving pulse.

DOI: 10.1103/PhysRevLett.92.047402

PACS numbers: 78.67.De, 03.67.-a, 42.65.Re, 73.21.Fg

Low-dimensional semiconductors are important model systems for studying quantum coherences in electron plasmas. In future schemes based on quantum information processing [1], the phase of the material polarization and the connected electromagnetic field carry information. Thus far, most experiments are based on a measurement of the populations of selected states after interaction with an external electromagnetic field [2–4]; i.e., they neglect the information contained in the coherent polarizations between quantum states [5].

Intersubband (IS) transitions in semiconductor quantum wells (QWs) are an interesting model system for optical polarization control [6,7]. The quantum confinement of the electron wave functions along the *z* direction leads to the formation of subbands [Fig. 1(a)], between which dipole-allowed optical transitions occur at frequencies determined by the QW width. The nearly parallel in-plane dispersion of these subbands [Fig. 1(b)] leads to a transition frequency independent of the in-plane wave vector and thus to narrow IS absorption lines [Fig. 1(c)] in the midinfrared (MIR). Driving such a system coherently by femtosecond MIR pulses, i.e., generating a quantum mechanical superposition of the envelope wave functions of the optically coupled subbands, allows for controlling optical polarizations [8].

In this Letter, we present a novel scheme to generate and measure coherent polarizations in real time up to frequencies of 30 THz. We demonstrate for the first time Rabi oscillations [9] on IS transitions of electrons in GaAs/AlGaAs quantum wells. The transient IS polarization is fully characterized by time-resolved measurements of the instantaneous electric field coherently emitted by the sample. The emitted field reveals a pronounced influence of many-body effects on the polarization dynamics. Our results directly show the possibility to control and measure such coherent polarizations despite their subpicosecond decoherence times.

The basic concept of our experiment is shown in Fig. 1(d). A coherent IS excitation is created by a femtosecond MIR pulse with a center frequency resonant to the

1 ↔ 2 IS transition [Fig. 1(c)]. The incident excitation pulse and the light emitted by the sample are fully characterized by measuring their amplitude and phase. Experiments were performed for different field strengths of the excitation pulses.

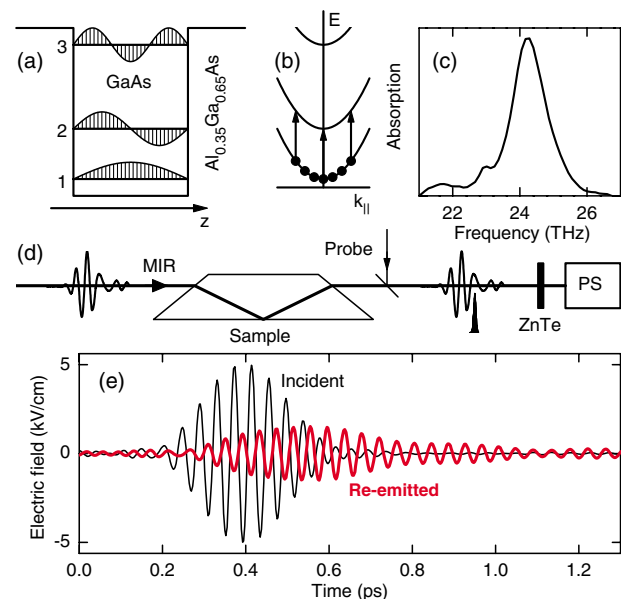


FIG. 1 (color online). (a) Envelope wave functions (simplified) of an electron confined in the potential well made by the different conduction band edges of GaAs (wells) and $\text{Al}_{0.35}\text{Ga}_{0.65}\text{As}$ (barriers). (b) The dispersions of the subbands are almost parallel along the in-plane wave vector k_{\parallel} . (c) Stationary IS absorption. (d) Schematic of the time-resolved nonlinear propagation experiment: An intense MIR pulse is sent through the prism-shaped sample. The electric field of the transmitted light induces in a thin ZnTe crystal a time-dependent birefringence, which is temporally sampled using a 12-fs probe pulse and a polarization sensitive detector (PS). (e) Measured coherent linear response of the IS transition. Thin line: incident field $E_{\text{in}}(t)$; thick line: reemitted transient $E_{\text{em}}(t)$ from the sample.

Midinfrared pulses with durations of 200 fs and electric-field amplitudes of up to 1 MV/cm are generated via difference frequency mixing of intense 25-fs pulses at 800 nm in GaSe [10]. We investigated an n -type modulation-doped QW sample consisting of 51 GaAs QWs of 10-nm width, separated by 20-nm-thick $\text{Al}_{0.35}\text{Ga}_{0.65}\text{As}$ barriers, the centers of which are doped with Si, resulting in an electron concentration of $n_s = 5 \times 10^{10} \text{ cm}^{-2}$ per QW. The Fermi energy is much smaller than the subband separation so that only subband 1 is populated. The 1 THz-wide [FWHM, Fig. 1(c)] $1 \leftrightarrow 2$ IS absorption line is homogeneously broadened and has a decoherence time of 320 fs [11]. The sample was processed into a prism [Fig. 1(d)] to achieve a strong coupling of the p -polarized MIR pulse and the IS transition dipoles. Experiments are performed at a sample temperature of 100 K. For measuring the MIR electric field by electro-optic sampling [12], the MIR transient is combined with a near-infrared (800 nm) 12-fs probe pulse. Both are focused onto a 10- μm -thick (110)-oriented ZnTe crystal. The electro-optic modulation induced by the ultrafast Pockels effect leads to a polarization change of the probe pulse proportional to the momentary MIR electric field. This signal is measured using a polarization sensor [PS in Fig. 1(d)] [10]. By varying the time delay between the MIR transient and the probe pulse, the temporal waveform of the MIR transient is sampled directly.

We first study the coherent response of the sample in the linear regime, i.e., for electric-field amplitudes of the excitation pulse below 5 kV/cm. Figure 1(e) shows the time-resolved incident field $E_{\text{in}}(t)$ at the position of the quantum wells (located at the base of the prism), as derived from a measurement of the pulse sent through an undoped reference sample of identical prism shape to compensate for the delay and the small dispersion introduced by the substrate of the sample (for details see [7]). The thick line represents the coherent emission $E_{\text{em}}(t)$ from the sample, which is given by the field $E_{\text{tr}}(t)$ transmitted through the sample minus the incident field $E_{\text{in}}(t)$.

The reemitted light reflects the free induction decay of the excited coherent IS polarization, a behavior characteristic for linear resonant absorption of a two-level system: Driven by the excitation field $E_{\text{in}}(t)$, a macroscopic linear coherent IS polarization $P(t)$ builds up gradually in the sample. In the case of exact resonance, this polarization is 90° out of phase with the driving field. Maxwell's equations with a coherent polarization source located in a thin δ -like layer [13,14] predict that the reemitted field $E_{\text{em}}(t)$ from the sample is proportional to the time derivative of $P(t)$, i.e., another 90° out of phase with $P(t)$. Both phase shifts together result in $E_{\text{em}}(t)$ being 180° out of phase with $E_{\text{in}}(t)$ as clearly observed in our experiment [Fig. 1(e)]. For $t > 0.6$ ps, $P(t)$ and concomitantly $E_{\text{em}}(t)$ decay with the decoherence time $T_2 = 320$ fs of the macroscopic IS polarization [11].

The amplitude and the phase of the reemitted light change dramatically for amplitudes of $E_{\text{in}}(t)$ above 10 kV/cm. In Figs. 2(a)–2(c), we show $E_{\text{in}}(t)$ and $E_{\text{em}}(t)$ for three different amplitudes of $E_{\text{in}}(t)$. For an amplitude of 20 kV/cm [Fig. 2(a)], the emitted field $E_{\text{em}}(t)$ is still out of phase with $E_{\text{in}}(t)$ but its amplitude rises faster than in the linear case, reaches a maximum together with $E_{\text{in}}(t)$, and eventually decays almost completely within the time of the driving pulse. For a driving field amplitude of 30 kV/cm [Fig. 2(b)], one finds at early times $t < 0.45$ ps an even faster rise and decay of $E_{\text{em}}(t)$, which is *out of phase* with $E_{\text{in}}(t)$. At $t = 0.45$ ps, the amplitude of $E_{\text{em}}(t)$ almost vanishes. In the second half of the driving pulse, we observe a second rise and decay of $E_{\text{em}}(t)$ which is, however, *in phase* with the driving

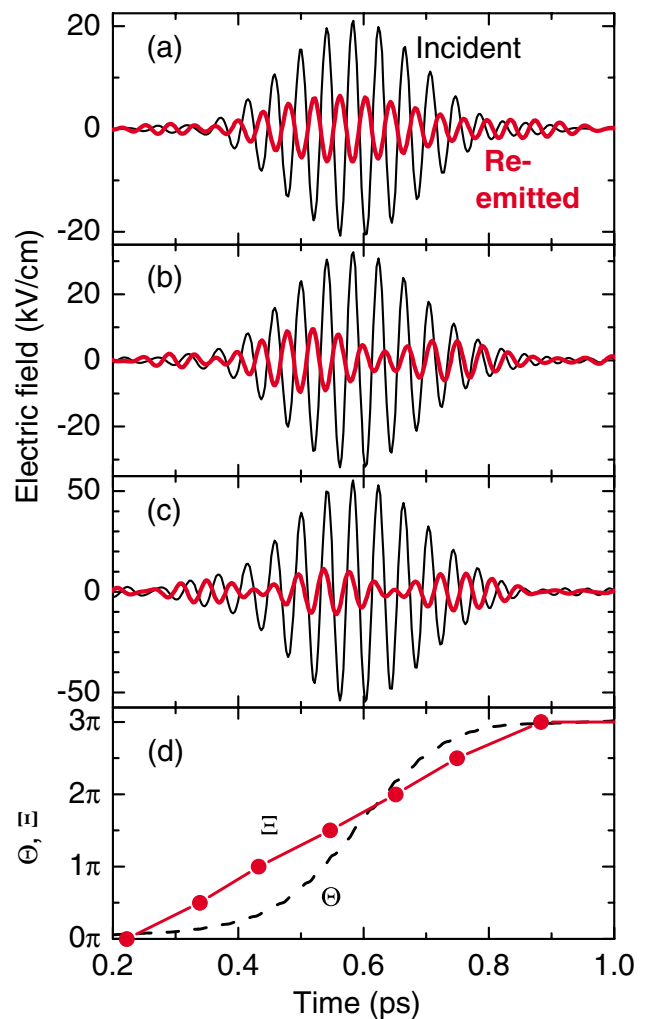


FIG. 2 (color online). (a)–(c) Ultrafast Rabi oscillations of the $1 \leftrightarrow 2$ IS transition measured as the coherent nonlinear response of the sample [reemitted field: $E_{\text{em}}(t)$ (thick lines)] to different strong incident electric fields $E_{\text{in}}(t)$ (thin lines). (d) Dashed line: pulse area Θ calculated from the incident electric field in (c). Dots: progress of the Rabi oscillation Ξ obtained from the envelope of the reemitted field.

field. For a driving field amplitude of 50 kV/cm [Fig. 2(c)], the periods of rise and decay of the reemitted field amplitude become even shorter, and we observe zero amplitudes at $t = 0.25$ ps and at $t = 0.45$ ps. The field $E_{em}(t)$ is first ($t < 0.25$ ps) out of phase with $E_{in}(t)$, for intermediate times ($0.25 \text{ ps} < t < 0.45 \text{ ps}$) in phase with $E_{in}(t)$, and finally ($t > 0.45$ ps) again out of phase with $E_{in}(t)$.

The data in Fig. 2 demonstrate that both amplitude and time structure of the macroscopic nonlinear polarization in the sample can be manipulated in a wide range by changing the strength of the coherent driving field. Our results are a direct manifestation of optical Rabi oscillations, which we observe directly through the nonlinear polarization, in contrast to studying population changes [2–4]. In the most elementary approach, Rabi oscillations of the polarization amplitude and of the population inversion are predicted by the Maxwell-Bloch equations for noninteracting two-level systems [13–15]:

$$\begin{aligned} \frac{\partial \rho_{12}}{\partial t} &= \left(i2\pi\nu - \frac{1}{T_2} \right) \rho_{12} + i\Omega(t)(1 - 2\rho_{22}), \\ \frac{\partial \rho_{22}}{\partial t} &= -\frac{1}{T_1} \rho_{22} + 2\Omega(t) \text{Im}(\rho_{12}), \\ P &= 2Nd \text{Re}(\rho_{12}), \quad E_{em} = -\frac{1}{2\epsilon_0 cn} \frac{\partial P}{\partial t}. \end{aligned} \quad (1)$$

The ρ_{ij} are the diagonal (populations) and off-diagonal elements (coherences) of the density matrix. They are damped by the phenomenological time constants T_1 and T_2 , respectively. $\Omega(t) = E_{in}(t)d/\hbar$ is the instantaneous Rabi frequency. The reemitted field $E_{em}(t)$ is proportional to the time derivative of the macroscopic polarization $P(t)$, which in turn is proportional to the electric dipole moment d and to the total sheet density N of coherently oscillating carriers. n contains the refractive index of the material surrounding the quantum wells and a factor correcting for the geometry of the experiment [14]. For absorption of light, the reemitted field transient $E_{em}(t)$ interferes destructively with the driving field $E_{in}(t)$, resulting in an attenuation of the transmitted field. For gain, constructive interference of $E_{em}(t)$ with $E_{in}(t)$ leads to amplification of the transmitted field.

The data in Figs. 1(e) and 2 are reproduced qualitatively by Eq. (1). In Fig. 3(a), the reemitted electric field $E_{em}(t)$ (thick lines) and the population $\rho_{22}(t)$ in the excited subband (shaded areas) are plotted for excitation in the linear regime [for simplicity we consider a driving field $E_{in}(t)$ with a rectangular amplitude in time and neglect any damping: $T_1 = T_2 = \infty$]. Such weak excitation leads to $E_{em}(t)$ being always out of phase with $E_{in}(t)$ and to an excited-state population that rises monotonically until the end of $E_{in}(t)$. A high driving field [Fig. 3(b)] leads to a Rabi oscillation of the excited-state population and to a reemitted field with a phase depending on the time derivative of the excited-state population $d\rho_{22}/dt$.

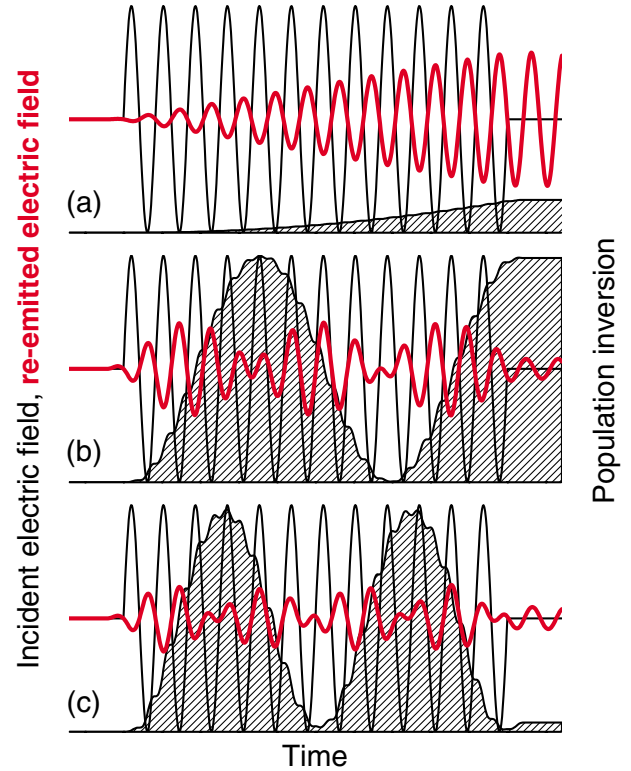


FIG. 3 (color online). (a),(b) Calculated time evolution of the reemitted field (thick lines) and the excited-state population (shaded areas) for an applied field (thin lines) using the Maxwell-Bloch equations [Eq. (1)] for uncoupled two-level systems. (c) For the same field amplitude as in (b), two coupled two-level systems lead to an increase of the Rabi frequency and to a decrease of the reemitted amplitude.

For $d\rho_{22}/dt > 0$ (period of light absorption), $E_{em}(t)$ is out of phase with $E_{in}(t)$. After reaching the population inversion, we have $d\rho_{22}/dt < 0$ (period of optical gain) and $E_{em}(t)$ in phase with $E_{in}(t)$. The experimental results of Fig. 2 show how the Rabi oscillations on the $1 \leftrightarrow 2$ IS transition change with the applied pulse area $\Theta = \frac{\pi}{2} \int |\Omega(t)| dt$ [16]. In Fig. 2(a), we observe a complete inversion of the IS transition when applying a driving field with pulse area $\Theta \approx \pi$. A stronger pulse with $\Theta \approx 2\pi$ [Fig. 2(b)] leads to complete population inversion around $t = 0.45$ ps, followed by a period of stimulated emission from inverted IS transitions until the end of the driving pulse. The situation in Fig. 2(c) strongly resembles the calculated result shown in Fig. 3(b) for a pulse with $\Theta \approx 3\pi$.

While Eq. (1) allows a qualitative description of our data, it is not sufficient for a quantitative description. The dashed line in Fig. 2(d) shows as a function of time the pulse area Θ calculated from the incident field. The dots give the pulse area Ξ derived from the measured progress of the Rabi oscillation: The maxima of the envelope of the reemitted field occur at Ξ equal to an odd multiple of $\pi/2$, the nodes at multiples of π . Equation (1) predicts $\Xi = \Theta$. At early times, Ξ and Θ differ by up to a factor

of 4, a clear indication that the simple Bloch picture fails in our case.

Such discrepancy can result either from a local electric field modifying $E_{in}(t)$, or from a time-dependent dipole moment $d(t)$. Local field effects could originate from radiative coupling [13,17–19]; i.e., the local electric field in a particular QW consists of the externally applied field $E_{in}(t)$ plus the reemitted fields from all QWs. Calculations of radiative coupling show [20] that in our sample this effect has a negligible influence on $\Omega(t)$.

A dipole moment d larger than expected in a single particle approach occurs if m QW electrons are coupled to form a collective excitation, the IS plasmon [21]. The dipole moment of this quasiparticle is larger than the dipole moment of a single electron by a factor of \sqrt{m} . On the other hand, the density of dipoles N decreases by a factor of m . The IS plasmon and m independent electrons give rise to the same linear absorption strength: The linear susceptibility scales as Nd^2 , so that the decrease of N exactly cancels the increase of d . Nonlinear experiments, however, can distinguish between the two types of excitations, as $\Omega(t)$ depends only on d , but not on N .

To illustrate the effect of coupled QW electrons, we consider the simplest case, $m = 2$. This corresponds to four states, $|11\rangle$ (both electrons in the ground state 1, energy 0), $|12\rangle$, $|21\rangle$ (one electron in 1, the other in the excited state 2, energy $h\nu$), and $|22\rangle$ (both electrons in 2, energy $2h\nu$). A coupling H_C with the matrix elements $\langle 12|H_C|21\rangle = \langle 21|H_C|12\rangle = C$ leads to two new quasiparticles at $h\nu + |C|$ and $h\nu - |C|$. When the coupling $|C|$ is small compared to $|\hbar\Omega|$, the Bloch equations for this four-level system exactly reproduce the results of Eq. (1). For strong coupling, the dipole moment of the blueshifted transition increases by $\sqrt{2}$, whereas that of the redshifted one is zero. Thus, this simple model shows that a coupling between the IS dipoles leads to a field-dependent increase of the effective dipole moment. Figure 3(c) shows the effect of strong coupling on the Rabi oscillations for the same excitation field as in (b). Ξ increases from 3π without coupling [Fig. 3(b)] to 4.2π with strong coupling [Fig. 3(c)], corresponding to an increase of the Rabi frequency.

A coupling between the IS dipoles is caused by the Coulomb interaction between the QW electrons leading to the well-known depolarization shift [22], which is about 1 THz [23] in our sample. Since our model also predicts a frequency shift, we expect $|C|/h$ to be of the same order as the depolarization shift. The number m of coupled electrons can be estimated from the disorder potentials in the QWs caused by the doping atoms. Assuming randomly distributed donors, the typical length scale of potential fluctuations in the QW plane is 200 nm. Thus, one potential trough contains $m \approx 20$ electrons.

In Fig. 2(c), one observes a Rabi frequency that is nearly independent of the instantaneous $E_{in}(t)$. At early

and late times [small $E_{in}(t)$], the coupling $|C|$ is larger than $|\hbar\Omega|$ and the Rabi frequency is enhanced by the many-body effect. Around the maximum of the driving field, however, $|\hbar\Omega| > |C|$, resulting in a breakup of the Coulomb correlation. Such effects result in a measured Rabi frequency that is nearly constant during the driving pulse. A quantitative calculation of this behavior is beyond existing theories of many-body effects.

In conclusion, by the observation of Rabi oscillations we demonstrated coherent nonlinear optical control of polarizations and carrier populations in semiconductor quantum wells on ultrafast time scales. While two-level Bloch equations lead to a qualitative agreement with our results, it is necessary to include many-body interactions between the electrons for a quantitative agreement.

We acknowledge financial support by the Deutsche Forschungsgemeinschaft. C.W.L. is grateful for scholarships by the Deutscher Akademischer Austauschdienst and by the National Science Council of Taiwan. We thank I. Waldmüller and A. Knorr for performing calculations on the influence of radiative coupling.

*Permanent address: Department of Electrophysics, National Chiao Tung University, Hsinchu, Taiwan, Republic of China.

†Electronic address: reimann@mbi-berlin.de

- [1] C. Monroe, *Nature* (London) **416**, 238 (2002).
- [2] O. D. Mücke *et al.*, *Phys. Rev. Lett.* **87**, 057401 (2001).
- [3] S. T. Cundiff *et al.*, *Phys. Rev. Lett.* **73**, 1178 (1994).
- [4] T. H. Stievater *et al.*, *Phys. Rev. Lett.* **87**, 133603 (2001).
- [5] O. Golonzka *et al.*, *J. Chem. Phys.* **115**, 10 814 (2001).
- [6] J. N. Heyman, R. Kersting, and K. Unterrainer, *Appl. Phys. Lett.* **72**, 644 (1998).
- [7] F. Eickemeyer *et al.*, *Appl. Phys. Lett.* **79**, 165 (2001).
- [8] F. Capasso *et al.*, *Phys. Today* **55**, No. 5, 34 (2002).
- [9] I. I. Rabi, *Phys. Rev.* **51**, 652 (1937).
- [10] K. Reimann *et al.*, *Opt. Lett.* **28**, 471 (2003).
- [11] R. A. Kaindl *et al.*, *Phys. Rev. B* **63**, 161308 (2001).
- [12] Q. Wu and X.-C. Zhang, *Appl. Phys. Lett.* **71**, 1285 (1997).
- [13] T. Stroucken *et al.*, *Phys. Rev. B* **53**, 2026 (1996).
- [14] J. E. Sipe, *J. Opt. Soc. Am. B* **4**, 481 (1987).
- [15] F. Bloch, *Phys. Rev.* **70**, 460 (1946).
- [16] The factor of $\pi/2$ occurs because we do not use the pulse envelope, but rather the instantaneous electric field.
- [17] I. Waldmüller *et al.* (to be published).
- [18] I. Waldmüller *et al.*, *Phys. Status Solidi B* **238**, 474 (2003).
- [19] I. Waldmüller, J. Förstner, and A. Knorr, in *Nonequilibrium Physics at Short Time Scales*, edited by K. Morawetz (Springer-Verlag, Berlin, 2004), p. 251.
- [20] I. Waldmüller and A. Knorr (private communication).
- [21] J. B. Williams *et al.*, *Phys. Rev. Lett.* **87**, 037401 (2001).
- [22] D. E. Nikonov *et al.*, *Phys. Rev. Lett.* **79**, 4633 (1997).
- [23] S. Ernst *et al.*, *Phys. Rev. Lett.* **72**, 4029 (1994).